

Supplementary Materials

Regulating morphology of high-performance organic electrochemical transistors through a dual-solvent blade-coating strategy

Binglu Zhong^{1,#}, Jie Lu^{1,#}, Xingyu Jiang¹, Jie Wu¹, Dianjue Liu¹, Shaobo Ji¹, Zi Wang², Rui Zhang¹, Lizhen Huang^{1,*}, Lifeng Chi^{1,3}

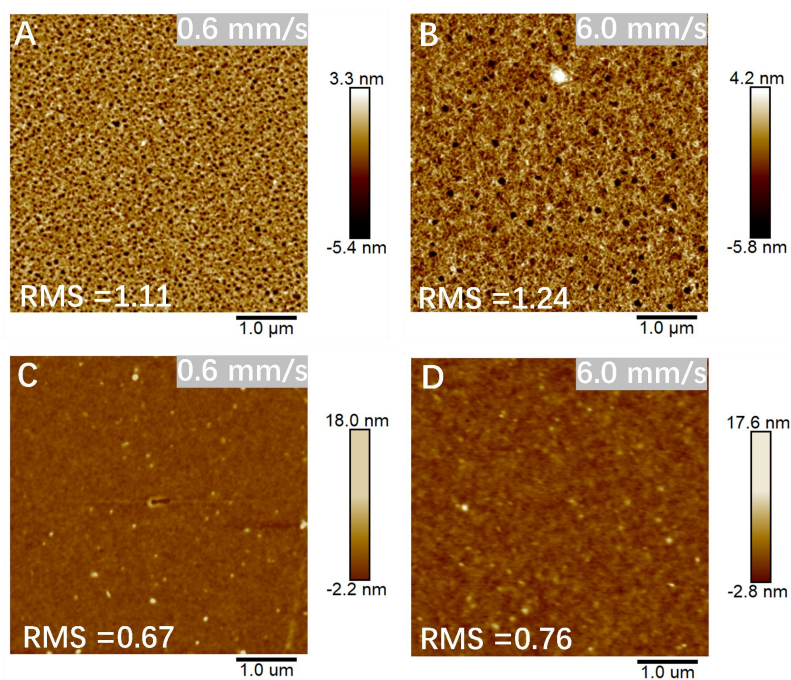
¹State Key Laboratory of Bioinspired Interfacial Materials Science, Institute of Functional Nano & Soft Materials (FUNSOM), Soochow University, Suzhou 215123, Jiangsu, China.

²Suzhou Laboratory, Suzhou 215123, Jiangsu, China.

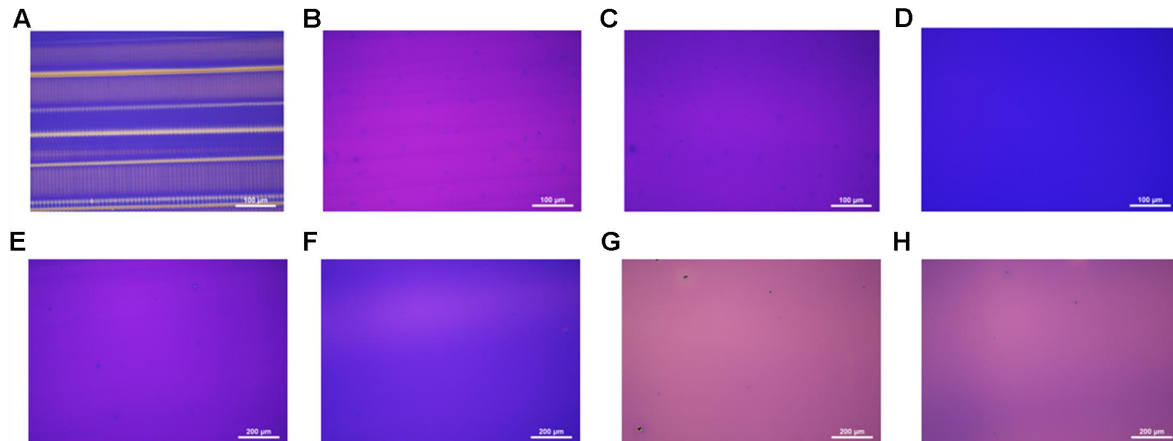
³Macao Institute of Materials Science and Engineering (MIMSE), MUST-SUDA Joint Research Center for Advanced Functional Materials, Macau University of Science and Technology, Macao 999078, China.

[#]These authors contributed equally to this work.

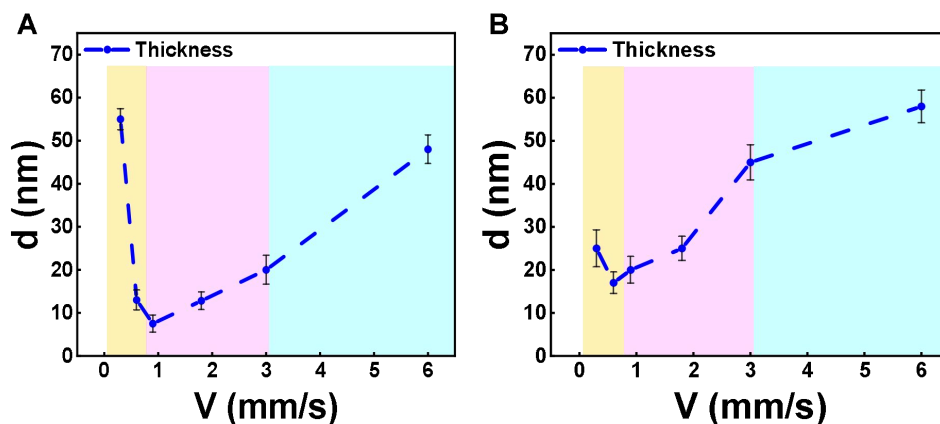
***Correspondence to:** Prof. Lizhen Huang, State Key Laboratory of Bioinspired Interfacial Materials Science, Institute of Functional Nano & Soft Materials (FUNSOM), Soochow University, Suzhou 215123, Jiangsu, China. E-mail: lzhuang@suda.edu.cn



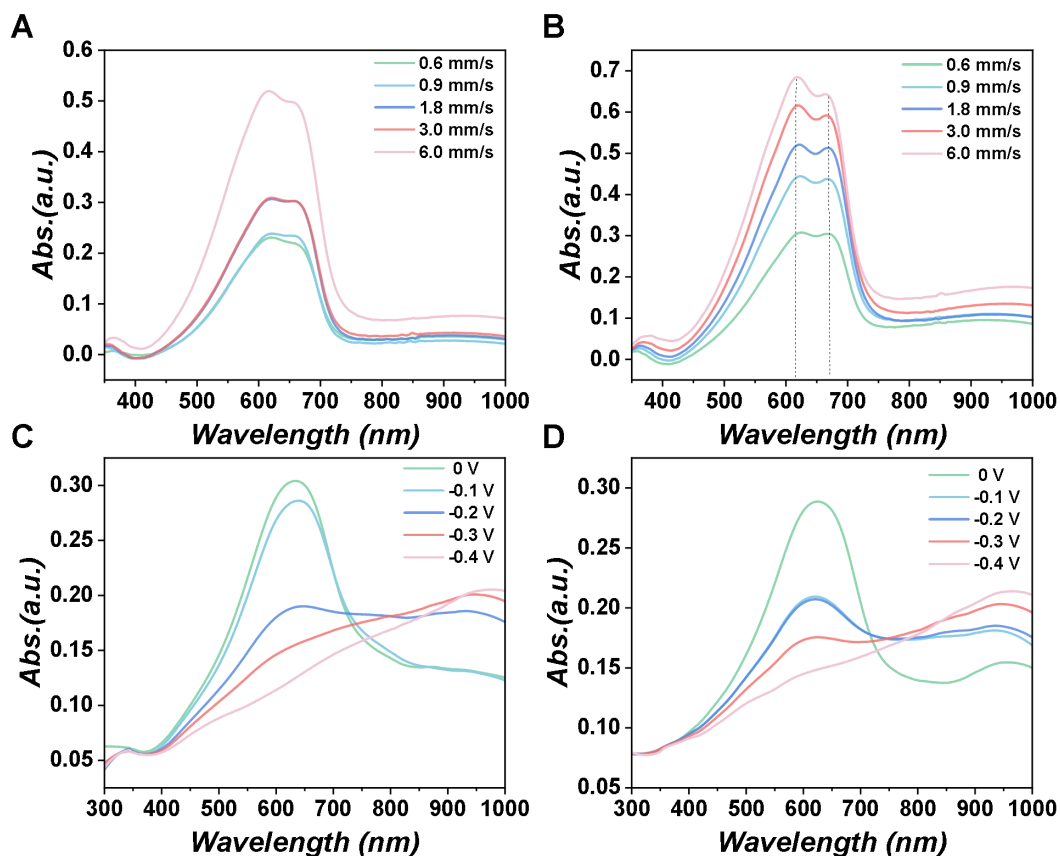
Supplementary Figure 1. (A)-(B) AFM morphology of single solvent blading coating at rates of 0.6 and 6.0 mm/s. (C)-(D) AFM morphology of dual solvent blading coating at rates of 0.6 and 6.0 mm/s.



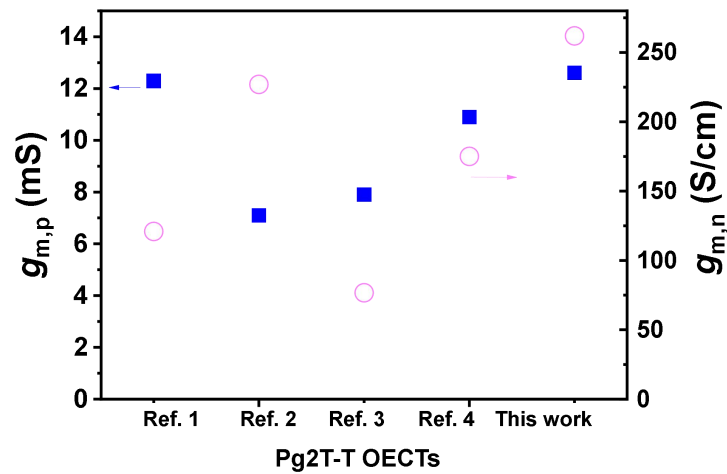
Supplementary Figure 2. (A)-(D) Optical image of single solvent chloroform 0.3, 0.9, 1.8, 3.0 mm/s. (E)-(H) Optical image of dual solvent chloroform 0.3, 0.9, 1.8, 3.0 mm/s.



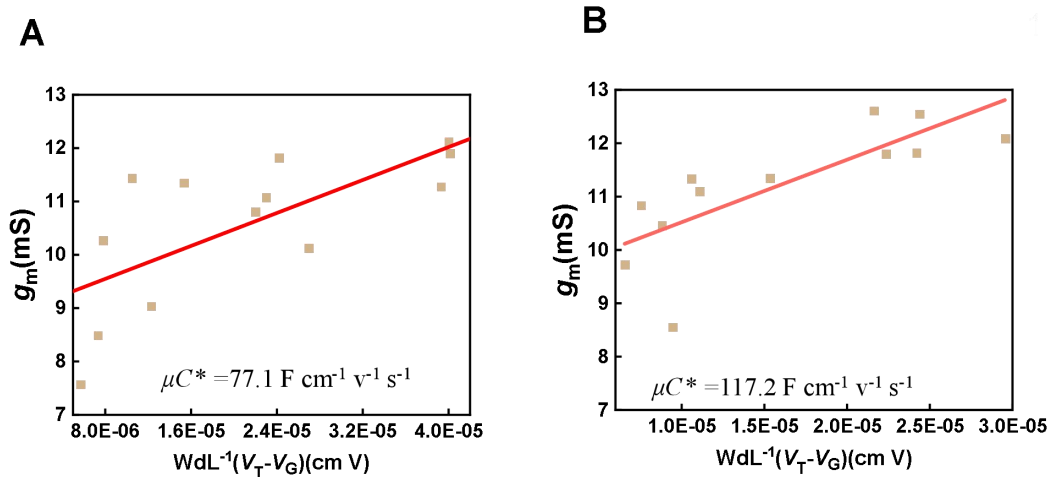
Supplementary Figure 3. (A) Diagram of single solvent film thickness variation with different rates. (B) Diagram of dual solvent film thickness variation with different rates.



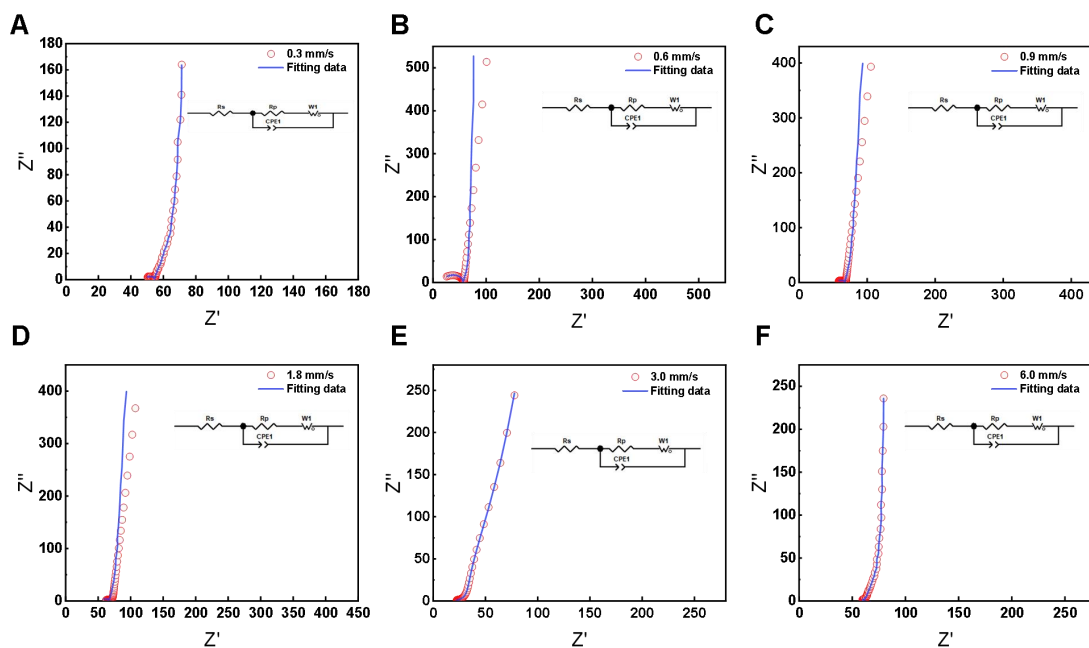
Supplementary Figure 4. UV-Vis-NIR absorption spectrum: (A) single solvent thin films at different rates in air. (B) dual solvent thin films at different rates in air. (C) The film with single solvent rate of 3.0 mm/s. (D) The film with dual solvent rate of 3.0 mm/s.



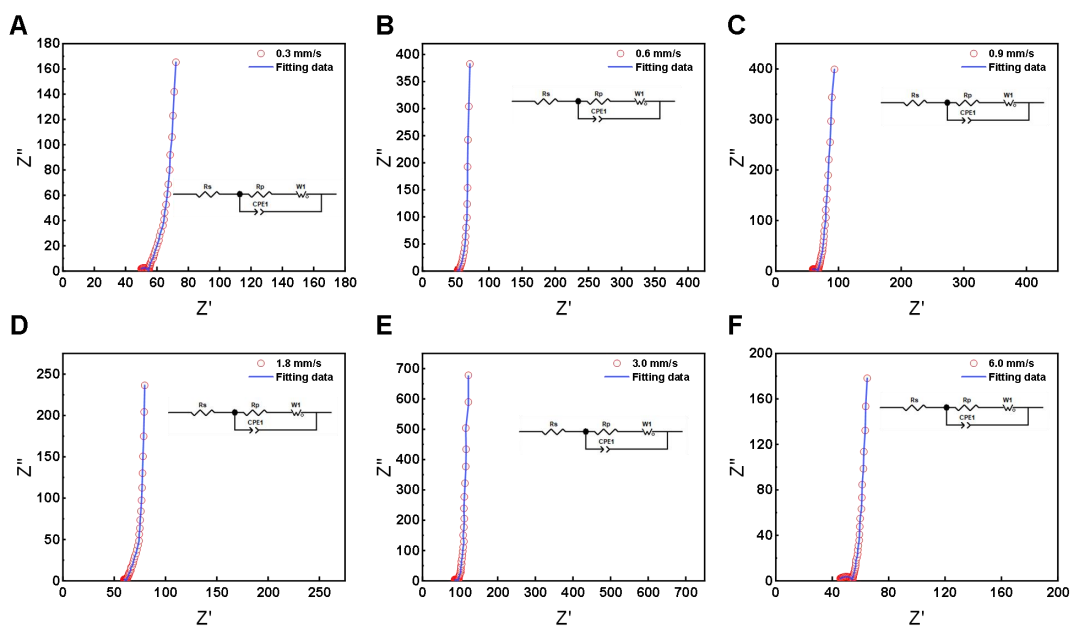
Supplementary Figure 5. Comparison of device performance ($g_{m,p}$ and $g_{m,n}$) in this work with previously reported literature.



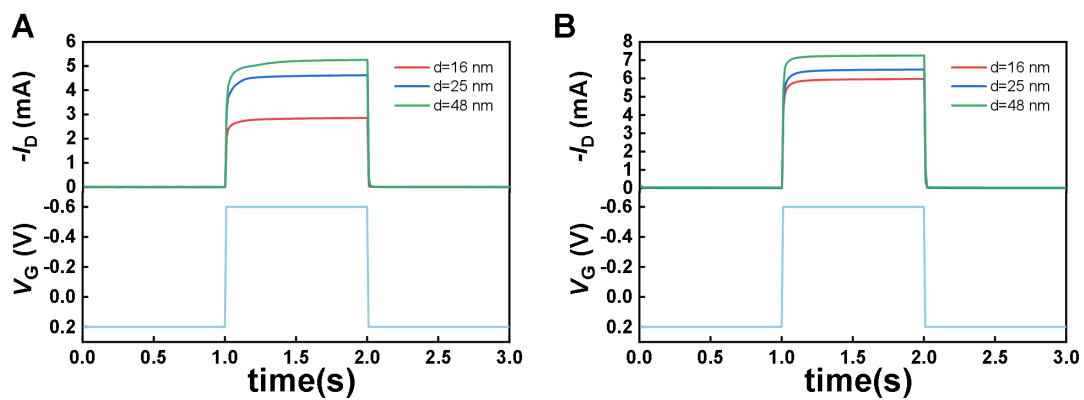
Supplementary Figure 6. (A) The μC^* values fitted from single solvent processed films with various thicknesses. (B) The μC^* values fitted from dual solvent processed films with various thicknesses.



Supplementary Figure 7. (A)-(F) Electrochemical impedance spectra of single solvent processed films at blading coating speeds ranging from 0.3 to 6.0 mm/s.



Supplementary Figure 8. (A)-(F) Electrochemical impedance spectra of dual solvent processed films at blading coating speeds ranging from 0.3 to 6.0 mm/s.



Supplementary Figure 9. (A)-(B) Turn-on time comparison of single (left) and dual (right) solvents at the same thickness of 16, 25, and 48 nm.

Supplementary Table 1. Electrical properties of OECTs ($W=100\ \mu\text{m}$, $L=10\ \mu\text{m}$) in single solvent and dual solvent at different shear rates.

Solvent	V (mm/s)	d (nm)	$g_{m,p}$ (mS)	μC^* ($\text{F cm}^{-1} \text{V}^{-1} \text{s}^{-1}$)	C^* (F cm^{-3})	μ ($\text{cm}^2 \text{V}^{-1} \text{s}^{-1}$)
Single solvent	0.3	55±5	10.13±1.36	306.9±33.5	204.5	1.5
	0.6	13±2	7.57±2.18	970.5±97.5	200	4.85
	0.9	7.5±2	5.41±1.67	1202.2±110.4	173.9	6.91
	1.8	16±3	8.49±1.26	884.4±55.4	233.8	3.78
	3	25±3	9.04±0.98	753.3±68.4	238.7	3.15
	6	48±3	11.18±0.52	388.2±43.3	201.8	1.92
Dual solvent	0.3	27±2	11.10±0.12	822.2±40.5	220.78	4.02
	0.6	16±2	10.46±0.32	1385.8±80.7	174.74	7.93
	0.9	20±2	9.73±1.01	1028.54±68.4	236.2	4.34
	1.8	25±3	11.34±0.35	1080±86.2	321.76	3.36
	3	48±4	12.61±0.60	457.57±67.4	238.98	1.91
	6	58±4	11.80±0.64	422.58±54.1	174.11	2.42

$g_{m,p}$ is the peak transconductance; W is the channel width; d is the thickness of the active layer; L is the channel length; μ is the charge-carrier mobility; C^* is the volumetric capacitance; V_T is the threshold voltage; V_G is the gate voltage.

μC^* is the quality factor calculated by the Equation (1)^[1].

Supplementary Table 2. Comparison of OECT performance ($g_{m,p}$ and $g_{m,n}$) of the devices in this study, and those in the literature.

Reference	Electrolyte	$g_{m,p}$ (mS)	$g_{m,n}$ (S/cm)	W/L (μm)	d (nm)
This work	0.1 M KCl	12.61	262.7	100/10	48
J. Mater. Chem. C. 2024,12, 7935–7942 ^[2]	0.1 M NaCl	12.29	121	200/10	52
Adv.Mater. 2021,33, 2007041 ^[3]	0.1 M KCl	7.1	227	100/10	50
J. Am. Chem. Soc. 2016,138,10252–10259 ^[4]	0.1 M NaCl	7.9	76.7	100/10	103
Adv. Electron. Mater. 2023,9, 2300119 ^[5]	0.1 M PBS	10.9	175.1	1500/50	20.75

REFERENCES

1. Ohayon, D.;Druet, V.;Inal, S. A guide for the characterization of organic electrochemical transistors and channel materials. *Chem. Soc. Rev.* **2023**,*52*, 1001-23. DOI: 10.1039/d2cs00920j
2. Li, M.;Feng, W.;Lan, Y; et al. Effects of selenium incorporation on the performance of polythiophene based organic electrochemical transistors. *J. Mater. Chem. C.* **2024**,*12*, 7935-42. DOI: 10.1039/d4tc01226g
3. Huang, L.;Wang, Z.;Chen, J; et al. Porous Semiconducting Polymers Enable High-Performance Electrochemical Transistors. *Adv. Mater.* **2021**,*33*, 2007041. DOI: 10.1002/adma.202007041
4. Nielsen, CB.;Giovannitti, A.;Sbircea, D-T; et al. Molecular Design of Semiconducting Polymers for High-Performance Organic Electrochemical Transistors. *J. Am. Chem. Soc.* **2016**,*138*, 10252-9. DOI: 10.1021/jacs.6b05280
5. Liu, C.;Deng, J.;Gao, L; et al. Multilayer Porous Polymer Films for High-Performance Stretchable Organic Electrochemical Transistors. *Adv. Electron. Mater.* **2023**,*9*, 2300119. DOI: 10.1002/aelm.202300119